

June 1986

LRP 295/86

**MULTIMODE SIMULATION OF THE FREQUENCY SPECTRUM
OF A QUASI-OPTICAL GYROTRON**

M.Q. Tran, A. Bondeson, A. Perrenoud,
S. Alberti, B. Isaak and P. Muggli

**MULTIMODE SIMULATION OF THE FREQUENCY SPECTRUM
OF A QUASI-OPTICAL GYROTRON**

M.Q. Tran, A. Bondeson*, A. Perrenoud,
S. Alberti, B. Isaak and P. Muggli

Centre de Recherches en Physique des Plasmas
Association Euratom - Confédération Suisse
Ecole Polytechnique Fédérale de Lausanne
21, Av. des Bains, CH-1007 Lausanne/Switzerland

* on leave from: Institute of Electromagnetic Field Theory
Chalmers University of Technology, Göteborg, Sweden,

ABSTRACT

We have performed a multimode simulation of the frequency spectrum of a quasi-optical 120 GHz gyrotron with a small mirror separation ($d = 5$ cm) which, therefore, presents a large separation between the frequencies of the modes ($\Delta\omega/\omega = 2.5\%$). It appears that under this condition multimode equilibrium is quite frequent. However, even if single mode equilibrium is not achieved, the electronic efficiency η remains high: under all magnetic field profiles its maximum reaches about 30%, and is equal to or exceeds the maximum single mode efficiency.

1. INTRODUCTION

The quasi-optical gyrotron is now being developed as an alternate concept for high power, millimeter wave source. In such devices, the electron beam interacts with the electromagnetic modes TEM_{mnq} of a quasi-optical resonator. While it is quite easy to select the transverse mode (usually the TEM_{00q}) by a suitable design of the resonator, the number of longitudinal modes which could be excited remains quite large due to the small separation between them. The question of the multimode evolution of a quasi-optical gyrotron has been first addressed by Bondeson et al. [1983], who showed that single mode equilibria could be obtained by a suitable choice of operating parameters. More recently [Quasi-Optical Gyrotron Development Group EPFL/BBC, 1985a and Perrenoud et al., 1986], we have developed a new resonator configuration which is frequency selective, and ensures a single mode operation even under conditions where it was reported not be attainable [Bondeson et al. 1983].

The previously published studies [Bondeson et al. 1983, Quasi-Optical Gyrotron Development Group EPFL/BBC, 1985a and Perrenoud et al. 1986] are pertinent to a quasi-optical gyrotron with a large mirror separation: the separation $\Delta\omega$ between two neighbouring modes is much less than the operating frequency ω (typically $\Delta\omega/\omega \approx 3 \cdot 10^{-3}$) and the number of modes which can be excited is large (typically around 15-20). On the other hand, proof of principle experiments (Hargreaves et al. 1984, Quasi-Optical Gyrotron Development Group 1985b) of the quasi-optical gyrotron are usually performed with small resonators to avoid the mode competition problem. For a gyrotron operating at

120 GHz and having a mirror separation d of 5 cm, two neighbouring modes are separated by 3 GHz and only 3 of them can be excited. Therefore, the mode competition has been considered not to be important and has not been studied previously. We wish to report here on numerical simulations on the multimode evolution for the small resonator of our quasi-optical gyrotron [Quasi-Optical Gyrotron Development Group 1985b]. It is found that depending on the magnetic field value and profile, either single mode or two mode equilibria could be obtained. In all cases, an efficiency equal or even higher than the optimum single mode one is obtained.

The paper is organized as follows: In Section 2, a brief description of the relevant parameters of our 120 GHz gyrotron will be presented. The results of the numerical simulation will be presented in Section 3 and will be discussed in the last one.

2. THE QUASI-OPTICAL GYROTRON PARAMETERS

The quasi-optical gyrotron which is under development at the Centre de Recherches en Physique des Plasmas [Quasi-Optical Gyrotron Development Group 1985b] is designed to operate at 120 GHz at a power level of 200 kW and with a pulse length up to 100 ms. In the first experiments, the pulse length will be limited to less than 1 ms. Such an operation is compatible with the use of a small resonator formed by two confocal mirrors separated by a distance d of 5 cm. The power transmission T is equal to 2%, which corresponds to a quality factor of 12570. The spot size $r_0 = (\lambda d / 2\pi)^{1/2}$ is 0.45 cm.

The electron beam is generated by a magnetron injection gun. Its parameters in the focal spot of the resonator are given in Table I. Its annular geometry renders the problem of its position with respect to the centre of the resonator important as far as the optimization of the efficiency is concerned. In the linear regime the annular beam efficiency (η_a) is related [Bondeson et al. 1983] to the pencil beam efficiency (η_p) by :

$$\frac{\eta_a}{\eta_p} = \frac{1}{2} \left[1 \pm J_0(2kr_b) \right] \quad (1)$$

where J_0 is the Bessel function of order 0, $k = 2\pi/\lambda$ is the wave-number and r_b the mean beam radius: the sign - corresponds to a beam centred at a field node and + at a maximum (Fig. 1). Due to technological constraints on the electron gun cathode, we have chosen the second minimum of J_0 ($kr_b = 5.087$). The ratio η_a/η_p is 0.625 when the beam is centred at a node and 0.375 in the other situation.

The frequencies of TEM_{00q} modes in an open confocal resonator are given by :

$$f = \frac{c}{2d} \left[q + \frac{1}{2} \right] \quad (2)$$

We choose d such that the resonant frequency of the TEM_{0040} is 120 GHz. At the centre of the resonator the rf electric field has a node for even q modes, and a maximum for odd q mode. Thus the TEM_{0038} , TEM_{0040} and TEM_{0042} will have a better coupling and a larger efficiency than the ones with odd values of q ($q = 39, 41$). The starting current for the various modes is presented in Fig. 2. In this cal-

ulation the fact that the resonator transmission depends slightly on the mode number is taken into account.

3. NUMERICAL SIMULATION

A numerical study of the frequency spectrum of the output of the gyrotron has been performed using the multimode code developed by Bondeson et al. [1983]. The code has now been optimized for efficient execution in the Cray 1-S computer recently installed at the Ecole Polytechnique Fédérale de Lausanne. It allows to follow the time evolution of the non-linearly coupled TEM_{00q} modes of a quasi-optical gyrotron, for a given magnetic field value and profile, output transmission factor T and beam current I . In this simulation, five TEM_{00q} modes were considered ($q = 37, 38, 39, 40, 41$). The frequency separation $\Delta\omega/\omega$ between two neighbour modes was set to 2.5%. The centre of the electron beam was placed at the centre of the cavity so that modes TEM_{0038} TEM_{0040} with even q have a better coupling with the beam as in the planned experiment. In all calculations T was fixed to 2% while two values of I were considered 4.5 A and 9 A.

Three cases of magnetic field profiles were considered: a flat one, a linearly down-tapered one ($\Delta B/B = -6\%$ across $4 r_0$) and a linearly up-tapered one ($\Delta B/B = +6\%$ over $4 r_0$). All through the paper, the magnetic field gradient $\Delta B/B$ will be defined as:

$$\frac{\Delta B}{B} = \frac{B(z; +2r_0) - B(z; -2r_0)}{B(z; 0)} \quad (3)$$

and thus gives the variation of the B-field across $4 r_0$.

Note that in our experiment, the field gradient is limited to $\Delta B/B = 1\%$ per centimetre for an operation of the gyrotron at 120 GHz [Spoorenberg et al., 1985] and only the flat field profile could be realized experimentally at 120 GHz. In the three cases, the magnetic field B_0 at the centre of the resonator has been varied and its influence over the output frequency spectrum studied. It usually takes between 100 to 300 time steps, i.e. between 600 ns and 1900 ns, to reach an equilibrium. The normalized time \hat{t} is related to the physical time t by (cf. the footnote)

$$t = \hat{t} \frac{mc^2}{e} \frac{\epsilon_0 d}{4I} \quad (4)$$

At time $\hat{t} = 0$, the electron beam with the ratio $p_{\perp}/p_{\parallel} = 1.5$ is switched on.

The definition of the normalized time t in page 330 of the paper of Bondeson et al. [1983] should be corrected as follows:

$$t = \hat{t} \frac{mc^2}{e} \frac{\epsilon_0 d}{4I} = \hat{t} \tau \frac{170}{I}$$

where d is the mirror spacing and I the beam current. Therefore for a 5 cm cavity and a 10 A-beam, one time step t corresponds to 5.6 ns.

The initial normalised amplitude \hat{E} of the five modes were equal to $5 \cdot 10^{-4}$ and their relative phases were random. The normalisation of the electric field is given by

$$\hat{E} = \frac{\sqrt{\pi} e E r_0}{m c^2} \quad (5)$$

where E is the peak value of the electric field at the centre of the interaction region. For our parameters $\hat{E} = 0.1$ corresponds to an electric field of 6.43 MV/m.

The sensitivity of the simulations to the initial condition has been checked by changing the initial value of \hat{E} ($\hat{E} = 10^{-4}$) or the initial phases. No significant changes in the frequency spectrum or the electric efficiency were obtained.

3.1 Flat Magnetic Profile

The simulation was run for a beam current of 9 A and the ratio Ω/ω of the non-relativistic cyclotron frequency at the centre of the interaction region to the resonant frequency of the TEM_{0040} was varied between 1.045 and 1.090. Figure 3 shows that, except for Ω/ω equal to 1.045 and 1.090, the final equilibrium after 300 time steps (or in real time 1900 ns after switching on the electron beam) consists of two modes, the TEM_{0038} and TEM_{0039} for Ω/ω less than 1.070 and the TEM_{0039} and TEM_{0040} for Ω/ω larger than 1.070. The details of the frequency spectrum are shown in Fig. 4 together with the efficiency, at different magnetic fields. When the gyrotron oscillation stabilizes

to one mode ($\Omega/\omega = 1.090$ for the TEM_{0040} mode), the efficiency η is 25% and the amplitude of the electric field E is 0.45. These two values correspond to the one corresponding to the optimum operating point obtained from single mode calculation.

However, the maximum efficiency is not reached under these circumstances but rather when a two-mode equilibrium is set up ($\Omega/\omega = 1.070$ and 1.075): the maximum value of η is as high as 30%. For $\Omega/\omega = 1.075$, the amplitude of the TEM_{0039} and TEM_{0040} are 0.24 and 0.43. It is worth noting that the efficiency in this case is larger than under the optimum condition for a single mode equilibrium ($\Omega/\omega = 1.090$), although in both cases the amplitude of the TEM_{0040} is comparable. This indicates that the presence of TEM_{0039} enhances the efficiency.

A typical time evolution of the various modes is shown on Figs. 5 and 6. In Figure 5, the ratio Ω/ω is equal to 1.095 so that a single mode equilibrium is obtained. At small time ($\hat{t} < 5$), both the TEM_{0039} and TEM_{0040} grow to roughly the same amplitude. The increase of the amplitude of the TEM_{0040} is then much faster: at $\hat{t} = 20$ it has practically reached its equilibrium value of $\hat{E} = 0.45$, while the amplitude \hat{E} of the TEM_{0039} is barely 0.074. The evolution towards a single mode equilibrium is then much slower: at $\hat{t} = 300$, the electric field \hat{E} of the TEM_{0039} and TEM_{0040} is respectively 0.006 and 0.45. Changing now the ratio Ω/ω from 1.095 to 1.075 alters drastically the behaviour of the two modes (Fig. 6). Since the cyclotron frequency Ω is lower, the TEM_{0039} interacts better with the beam than the TEM_{0040} . However, one must not forget that this beneficial effect is

compensated by the averaging of the interaction along the annular electron (cf. § 2) which favours even modes. The combination of these two effects leads to a complex mode competition between the TEM_{0039} and TEM_{0040} . In the first phase ($t < 30$), TEM_{0039} grows faster than the TEM_{0040} and then decreases while the second mode keeps increasing. The process is relatively fast ($t < 100$) compared to the time required to reach a true single mode equilibrium ($t \approx 300$).

3.2 Down-tapered Magnetic Field Profile ($\Delta B/B = -6\%$)

A down-tapered magnetic field profile is usually imposed in order to keep the particles in resonance with the wave as they lose energy. As for the case of a flat profile and with a beam current of 9 A, two mode equilibria are obtained in the majority of the runs (Fig. 7). A maximum efficiency η of 28% is reached for a magnetic field at the centre of the resonator corresponding to $\Omega/\omega = 1.065$ (Fig. 8). Optimization performed with a single mode model yields an efficiency of 26% and Ω/ω of 1.071: both values are close to the one obtained from the multimode calculations.

Reducing the electron beam current to 4.5 A decreases the range where two modes equilibria are obtained (Fig. 9). The maximum efficiency is now reached when only the TEM_{0040} mode exists: η is 26% for $\Omega/\omega = 1.085$ and at a field amplitude of $E = 0.33$. The value of η is not strongly degraded when both the TEM_{0040} and TEM_{0039} are present: for example at Ω/ω is 1.075, η is 25% when the respective amplitude of the TEM_{0040} and TEM_{0039} are 0.3 and 0.1.

3.3 Up-tapered Magnetic Field Profile ($\Delta B/B = +6\%$)

The advantage of an up-tapered magnetic field profile is that it allows prebunching the electrons in the first region of the interaction region. According to the single mode optimisation, the single mode efficiency can be as high as 31% compared to 23% in the case of no-tapering and 26% for ($\Delta B/B = -6\%$).

The result of our calculations are summarized in Figs. 10 and 11. The electron beam current is set to 9 A. The same qualitative behaviour as for the two other field profiles is observed: two modes coexist for nearly all the magnetic fields (Fig. 10). The maximum efficiency ($\eta = 31\%$) occurs in presence of the two modes TEM_{0039} and TEM_{0040} for $\Omega/\omega = 1.075$ (Fig. 11). Decreasing the beam current to 4.5 A decreases the occurrence of multimode equilibria, as have been observed for a down-taper magnetic field profile.

4. DISCUSSION

The multimode simulation of a quasi-optical gyrotron having a small resonator ($\Delta\omega/\omega = 2.5\%$) shows that equilibria with two longitudinal modes occur for a wide variety of conditions. However, no degradation of the efficiency was found. In one case, the flat magnetic field profile, even the efficiency is higher than the one computed for single mode. Such a beneficial effect of having a two-mode equilibrium has already been noticed and discussed by Bondeson et al. [1983]:

in this paper two large amplitude modes separated by $\Delta\omega/\omega$ of about 2.5% yield an efficiency of 26% while the single-mode calculation only gives one of 14%.

A second point of interest is the relation between such numerical simulations and an experiment. No attempt has been made to incorporate in the code a realistic time evolution of the electron beam parameters. In an actual magnetron injection gun, neither the beam current nor the ratio p/p_{\parallel} are switched on instantaneously as it is assumed in the numerical simulations. Therefore, we do not claim here to predict the result of an actual experiment. We have rather studied the sensitivity of the final state of a complicated non-linear system to external conditions such as the magnetic field and the beam current. The time scale which can be inferred from the simulation should be considered only as indicative since the dynamics of the switching on of the electron beam may modify the excitation and evolution of the modes.

Albeit those remarks, it is interesting to compare qualitatively the predictions of the numerical simulations with the available experimental data obtained by Hargreaves et al. [1984] at the Naval Research Laboratory (NRL). No evidence of the simultaneous existence of two modes was ever found. A few numerical simulations were performed with the parameters of the experiment: $\Delta\omega/\omega = 3.3\%$, $r_0 = 1.2$ cm, resonator quality factor $Q = 12500$, beam current $I = 10$ A, $\Delta B/B = \pm 5\%$ [Read, Private Communication]. The results are in agreement with the experimental findings: no multimode equilibria was found. It is

important to point out that the parameters of the NRL experiments differ strongly from ours. The frequency separation $\Delta\omega/\omega$ is larger (3.3% compared to 2.5%) and the interaction length $2 r_0$ is also longer (2.4 cm compared to 0.9 cm). Single-mode calculations have shown that due to the larger interaction length the efficiency η is more sensitive to the frequency detuning as measured by the dimensionless parameters $r_0(\Omega - \omega)/v_z$. Since the NRL experiment has both r_0 and $\Delta\omega$ larger than ours, it will be more difficult to excite two modes simultaneously. This qualitative argument explains the different behaviour between the NRL experimental result (and the corresponding simulations) and the numerical results performed for our experiment.

Acknowledgement

This work was partially supported by the "Commission pour l'Encouragement de la Recherche Scientifique".

We would like to acknowledge discussions with Dr. M.E. Read who has provided us with many details of the NRL experiments.

Electron beam parameters

Voltage V	70 kV
Max. current I	10 A
$P_{\perp} / P_{\parallel}$	1.5
Mean radius r_b	2.02 mm
$kr_b = 2\pi r_b / \lambda$	5.087

Table I

Electron beam parameters of the CRPP gyrotron

References

- BONDESON, A. MANHEIMER, W.M., and OTT, E., 1983, Multimode analysis of quasi-optical gyrotrons and gyroklystrons. *Infrared and Millimeter Waves*, 9, 309-339.
- HARGREAVES, T.A. KIM, K.J., McADOO, J.H., PARK, S.Y. SEELEY, R.D. and READ, M.E., 1984, Experimental study of a single-mode quasi-optical gyrotron. *Int. J. Electron.*, 57, 977-984.
- PERRENOUD, A., TRAN, M.Q., ISAAK, B., 1986, On the design of open resonators for quasi-optical gyrotrons. To be published in *Int. J. Infrared Millimeter Waves*.
- QUASI-OPTICAL GYROTRON DEVELOPMENT GROUP EPFL/BBC, 1985a, On the design of open resonators for quasi-optical gyrotrons. *Conf. Digest 10th Int. Conf. on Infrared and Millimeter Waves*, W.8.3.
- QUASI-OPTICAL GYROTRON DEVELOPMENT GROUP EPFL/BBC, 1985b, Design of a quasi-optical 120 GHz gyrotron. *Proc. of the Course and Workshop on Applications of RF wave to Tokamak Plasmas*, Varenna, 1985, edited by S. Bernabei, U. Gasparino and E. Sindoni, p. 848.
- SPOORENBERG, C.J.G., KRAALIJ, G.J., PIETERMAN, K., FRANKEN, W.M.P., TRAN, M.Q., 1985, A 5.0 Tesla superconducting magnet system for a gyrotron. *9th Int. Conf. Magnet Technology*, Poster 2PG-03.

Figures Captions

Fig. 1: Schematic of the position of the annular electron beam cross-section with respect to the electric field standing wave pattern in the resonator. Case (a) corresponds to a beam centred at a node of the electric field and case (b) at a maximum.

Fig. 2: Variation of the starting current of the various TEM_{00q} modes as a function of the magnetic field. The output transmission of the TEM_{0040} is 2%.

Fig. 3: Index q of the TEM_{00q} modes which are simultaneously excited when the magnetic field is varied. The field profile is flat ($\Delta B/B = 0$). At this high value of the electron beam current ($I = 9$ A), the equilibrium consists of two modes for nearly all values of Ω/ω .

Fig. 4: a) Amplitudes of the normalized field of different TEM_{00q} modes as function of the magnetic field ($I = 9$ A, $\Delta B/B = 0$).

b) Variation of the efficiency η as a function of Ω/ω . η as high as 29% is achieved in the presence of two modes and it exceeds the optimum efficiency obtained with only one mode.

Figures Captions (cont'd)

Fig. 5: Time evolution of the amplitude of the electric field of the TEM_{0039} and TEM_{0040} for $\Omega/\omega = 1.09$ and $\Delta B/B = 0$. The decay of the amplitude of the TEM_{0039} is very gentle and requires up to 300 time steps to reach a negligible value ($E < 10^{-2}$). The electric field of the TEM_{0040} remains at a constant high value for $t > 50$.

Fig. 6: Time evolution of the amplitude of the electric field of the TEM_{0039} and TEM_{0040} for $\Omega/\omega = 1.075$ and $\Delta B/B = 0$. The amplitude of both modes remains constant at larger times.

Fig. 7: Index q of the TEM_{00q} modes which are simultaneously excited in function of the magnetic field Ω . The field profile is down-tapered ($\Delta B/B = -6\%$). The cyclotron frequency Ω corresponds to the magnetic field at the centre of the resonator and ω the resonance frequency of the TEM_{0040} . The electron beam current I is 9 A.

Fig. 8: a) Amplitudes of the normalized electric field of different TEM_{00q} modes as function of the magnetic field ($\Delta B/B = -6\%$, $I = 9$ A).
b) Efficiency η as function of the magnetic field. Note that the highest efficiency is obtained when a two-mode equilibrium exists.

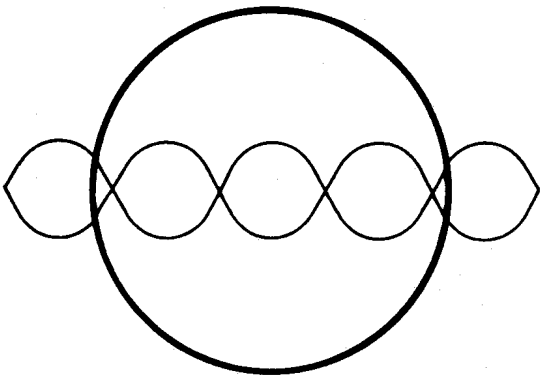
Figures Captions (cont'd)

Fig. 9: Index q of the TEM_{00q} modes which are simultaneously excited in function of the magnetic field ($\Delta B/B = -6\%$). The electron beam current I is 4.5 A. Compared to Fig. 7, the number of cases where a single mode equilibrium is reached, has greatly increased.

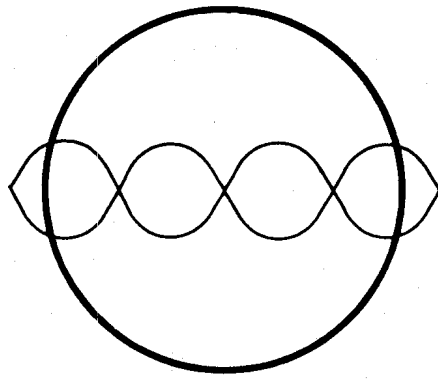
Fig. 10: Index q of the TEM_{00q} modes which are simultaneously excited in function of the magnetic field. The field profile is up-tapered ($\Delta B/B = +6\%$) and the electron beam current I is 9 A. The definition of Ω/ω is identical with that in Fig. 7.

Fig. 11: a) Amplitudes of the normalized electric field of different TEM_{00q} modes as function of the magnetic field ($\Delta B/B = +6\%$, $I = 9$ A).

b) Efficiency η as function of the magnetic field. For $\Omega/\omega = 1.07$, only the TEM_{0039} is excited. However, since the electron beam is centred at a maximum of the standing wave pattern (cf. Fig. 1a), the efficiency is reduced. High efficiency is obtained when two modes are excited.



(d)



(d)

Fig. 1

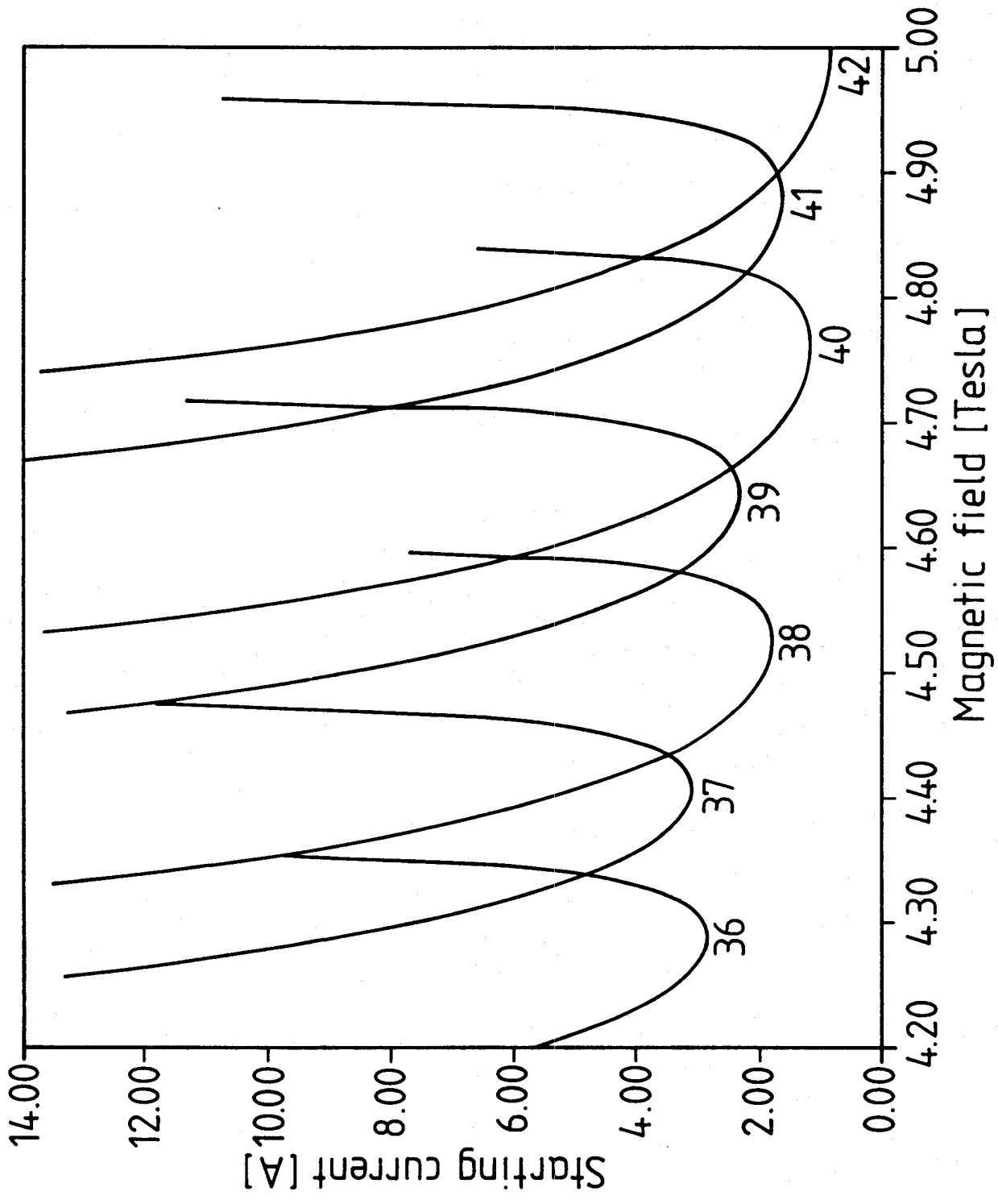


Fig. 2

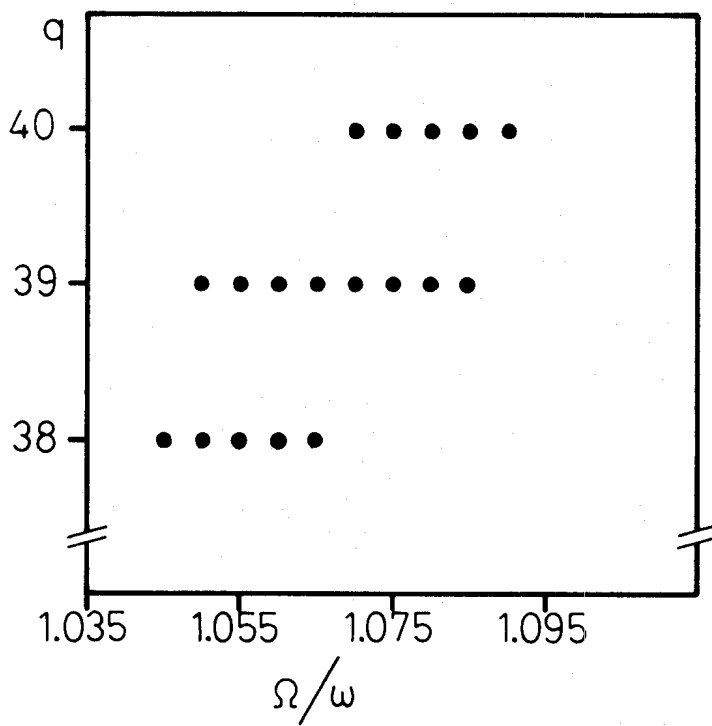


Fig. 3

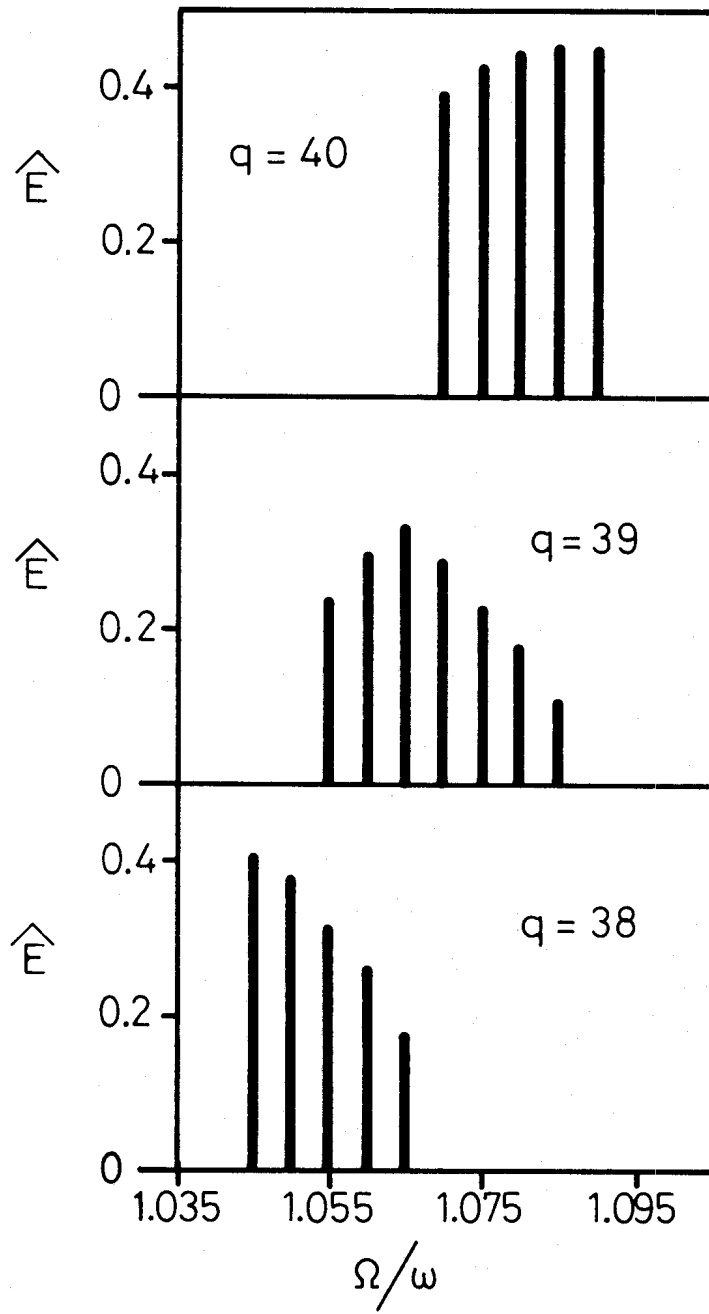


Fig. 4a

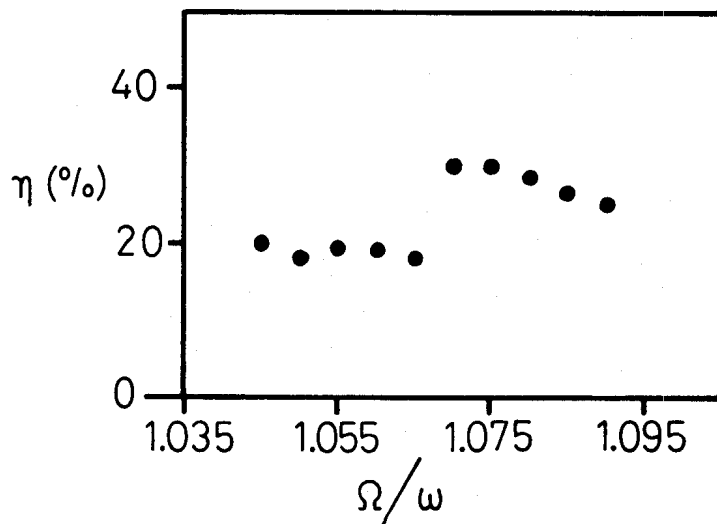


Fig. 4b

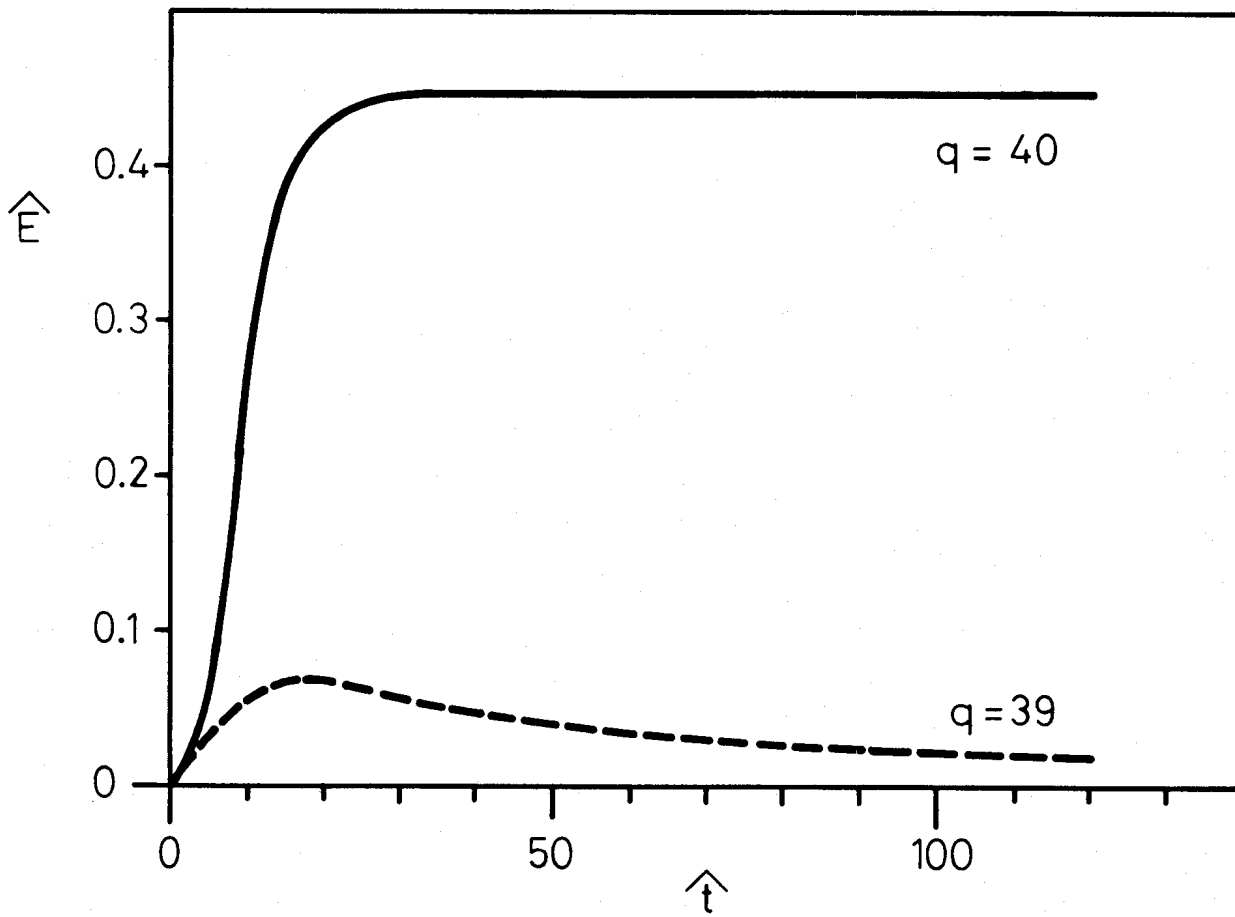


Fig. 5

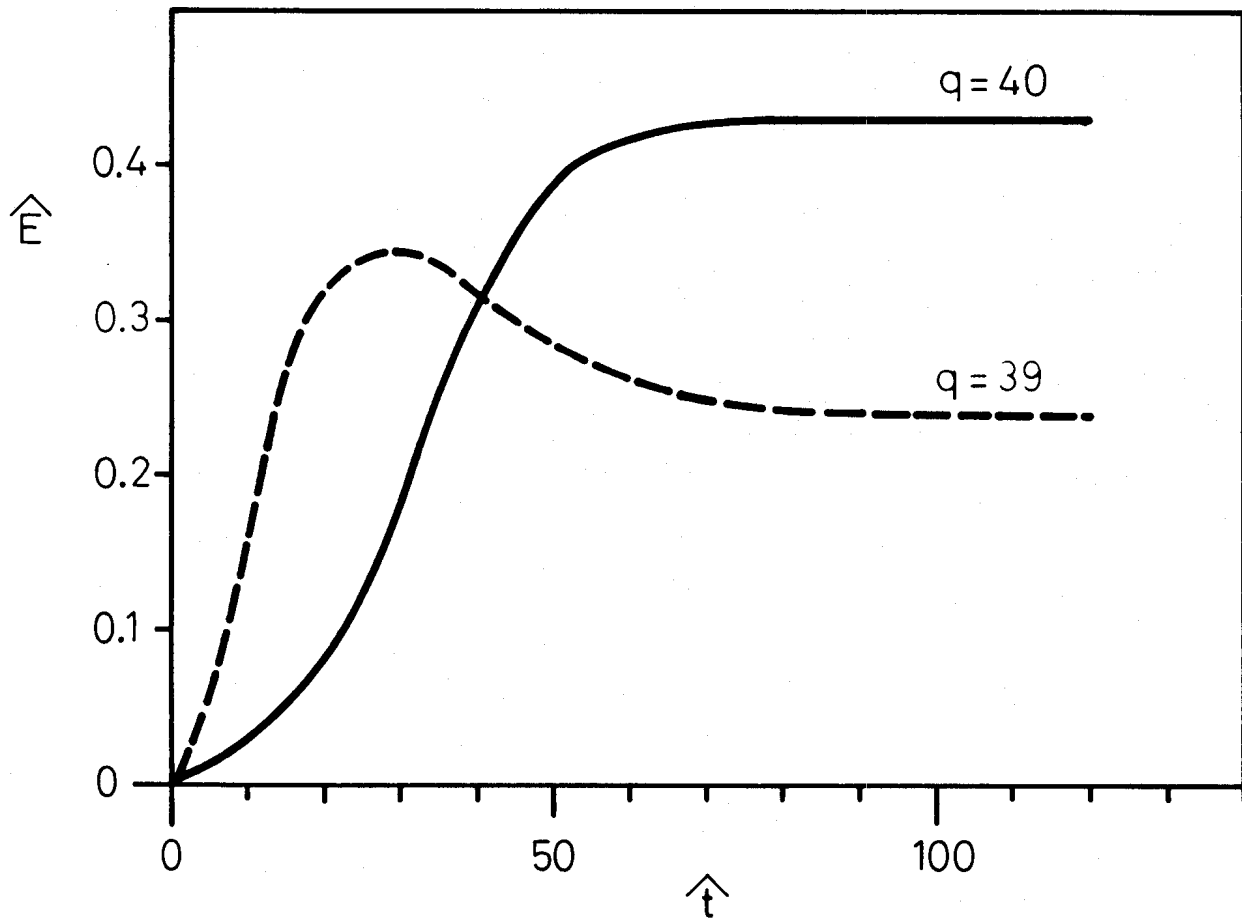


Fig. 6

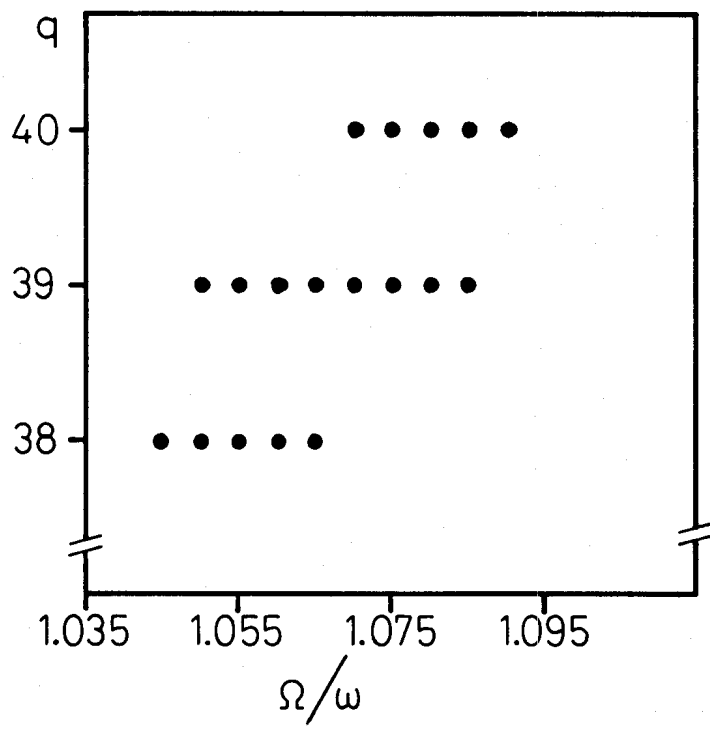


Fig. 7

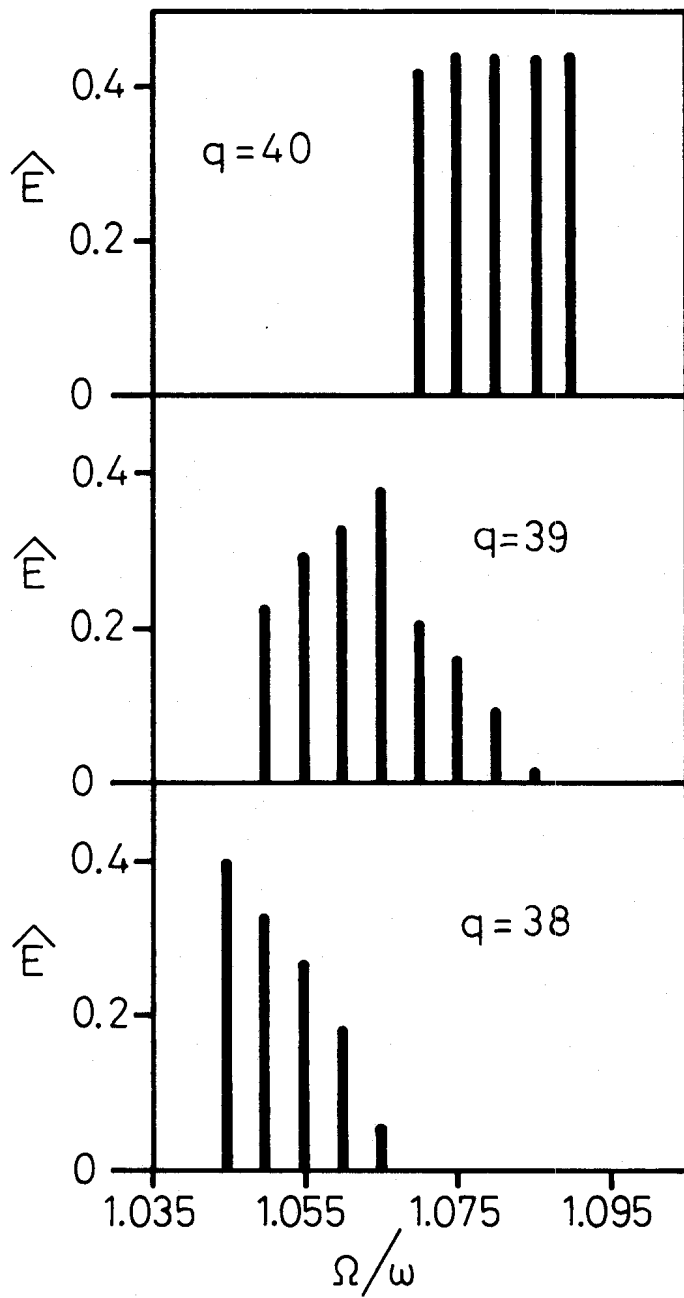


Fig. 8a

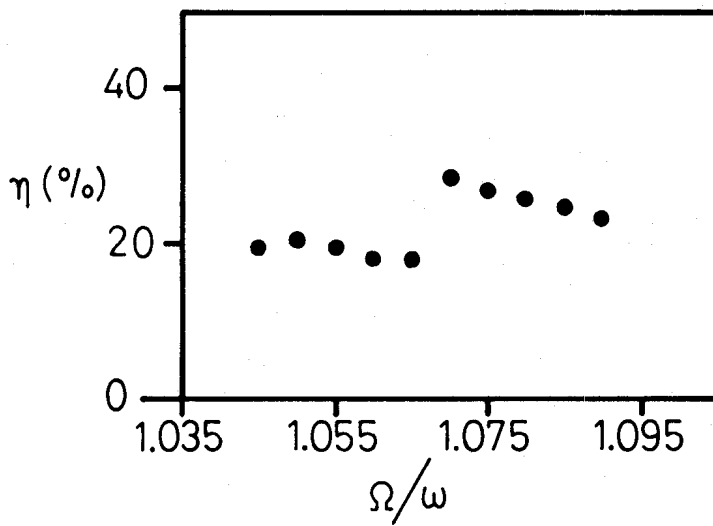


Fig. 8b

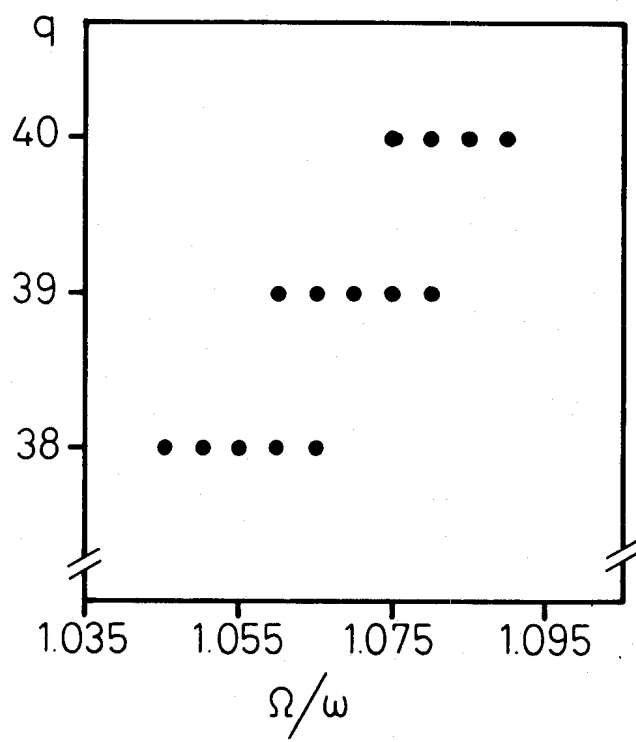


Fig.9

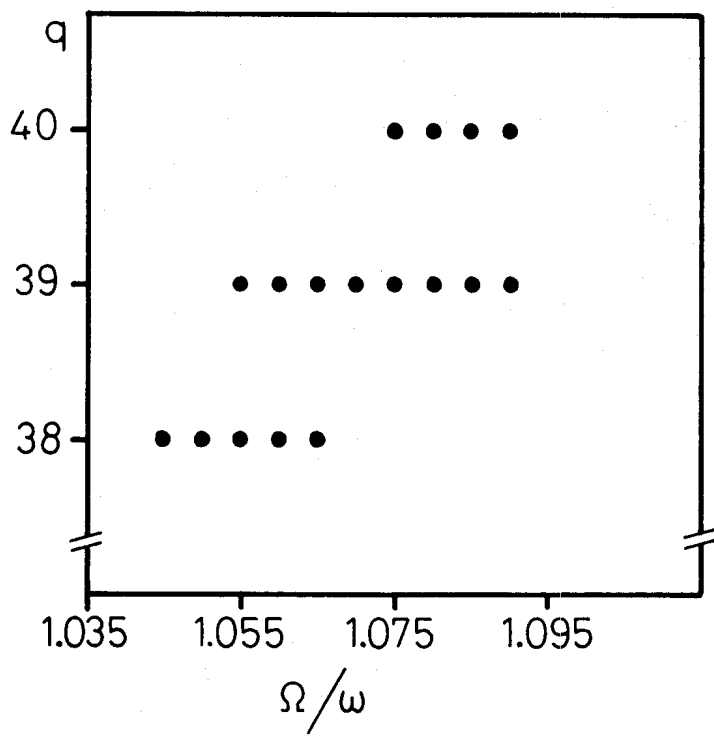


Fig.10

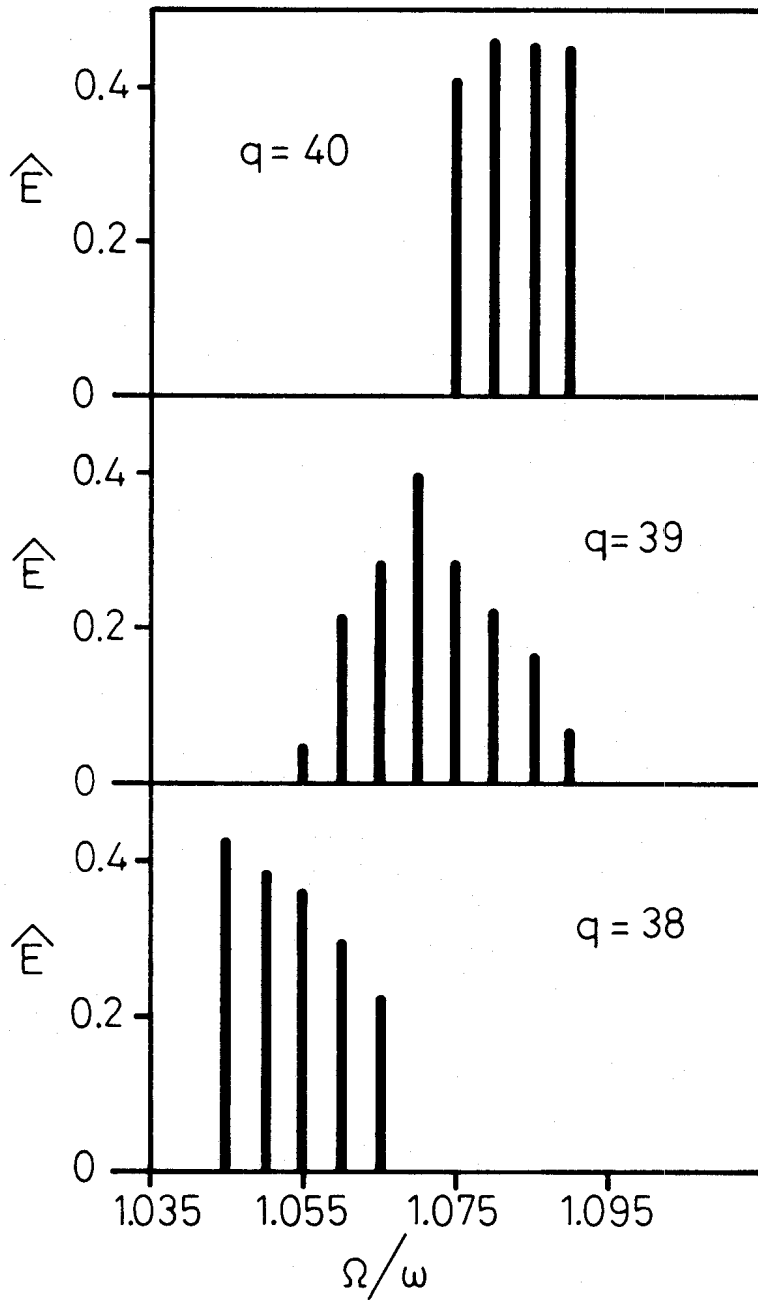


Fig.11a

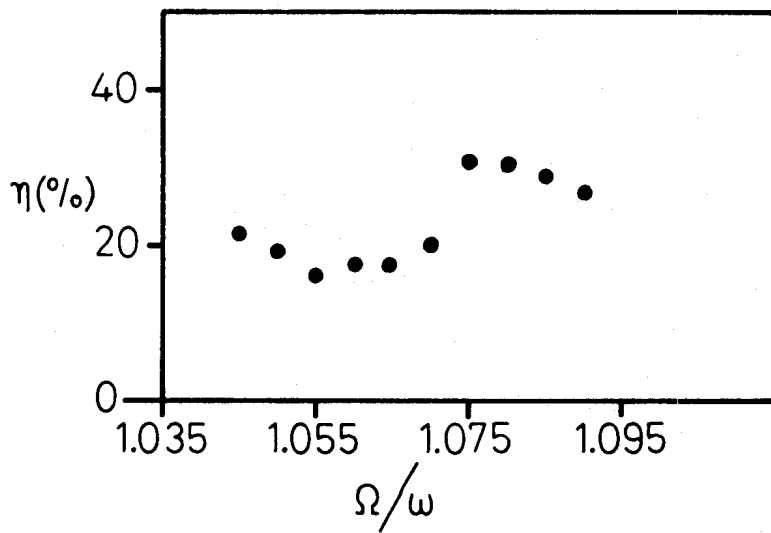


Fig.11b